

Morphological Characterization of Carbon-Nanofiber-Reinforced Epoxy Nanocomposites Using Ultra-Small Angle Scattering

Ryan S. Justice¹, David P. Anderson², Janis M. Brown³, Michael J. Arlen³, Amanda J. Colleary³, Khalid Lafdi², and Dale W. Schaefer^{1,4}

¹University of Cincinnati, Department of Chemical and Materials Engineering, Cincinnati, OH 45221-0012, USA.

²University of Dayton Research Institute, 300 College Park, Dayton, OH 45469-0168, USA.

³Air Force Research Laboratory, WPAFB, OH 45433-7750, USA.

⁴Manuel Lujan Jr. Neutron Scattering Center, Los Alamos National Laboratory, Los Alamos, NM 87545, USA.

INTRODUCTION

Studies of the properties of nanocomposites reinforced with vapor-grown carbon nanofibers (VGCFs) can be found throughout the literature.¹⁻⁵ Electrical, mechanical, viscoelastic, and rheological properties are just a few of the characteristics that have been well discussed.¹⁻⁵ Although these properties depend on *in situ* morphology, comprehensive morphological characterization is rare. Ultimately, the deficiency regarding filler and network characterization from a morphological perspective results from a lack of a reliable characterization technique that is widely accepted and easily accessible.

Due to its 2-dimensional nature, microscopy is of limited value when analyzing network morphologies for carbon nanofibers (CNFs). Optical microscopy, scanning electron microscopy, transmission electron microscopy, and Raman imaging/mapping all produce two-dimensional images. The filler network morphologies, however, are 3-dimensional; thus the characterization of these networks by two-dimensional techniques is flawed from the onset. Microscopy and scattering are complementary techniques and both are needed to sort out any complex morphology. Images serve to provide geometric constraints on other analytic techniques such as scattering.

In this work, we investigate the effects of nanofiber loading, fiber dimensions, and filler dispersion on the scattering profiles and electrical properties of CNF/Epon 862/CureW nanocomposites. Ultra-small angle x-ray scattering (USAXS) was used to characterize the morphology of carbon nanofibers suspended in epoxy. Using a simplified tube model, we estimate the dimensions of suspended fibers. The assumption of tubular fibers accounts for the increased surface area observed with USAXS that is not accounted for using a solid rod model. Furthermore, USAXS was used to search for a structural signature associated with the electrical percolation threshold. AC impedance spectroscopy was also employed to verify that an electrically conductive, percolated network developed.

EXPERIMENTAL

Sample Preparation. Pyrolytically stripped ASI carbon nanofiber (PR-19 LHT-LD) and 250-mL of reagent grade acetone (Aldrich chemical) were mixed using a high shear mixer running at 20,000 rpm for 1 hour. The samples were then sonicated using a 55-kHz bath sonicator for an additional 1 hour. Freshly mixed Epon862/Cure W resin was then

added and mixed with the high shear mixer for an additional 5 minutes. The acetone, nanofibers, and epoxy were placed in a vacuum oven overnight to remove the acetone.

In preparation for the curing process, the resin mixture was warmed and then poured into silicon molds designed to provide 1-mm thick samples. The molds were then covered with a flat silicon caul sheet and bagged for the autoclave. The samples were cured under vacuum at 100-psi and temperatures of 121°C (2 hours) and 177°C (2 hours). The composites remained in the autoclave until the system returned to ambient temperature.

Ultra Small Angle X-Ray Scattering. Scattering results from scattering-length density contrast between constituents and provides information about the three-dimensional arrangement of scattering objects. X-ray scattering at small angles is sensitive to large-scale inhomogeneities in electron density. Ultra-small angle scattering provides reliable information about real space structures ranging in size from 1-nm to a few mm. Structural information is gained by measuring the scattered intensity, I , as a function of scattering vector, q , which is related to the scattering angle (θ) by the following:

$$q = (4\pi/\lambda)\sin(\theta/2) \quad (\text{Eq. 1})$$

where λ is the wavelength of the radiation in the medium. The USAXS intensity is measured on an absolute scale as the differential scattering cross-section per unit sample volume, $I(q) = d\Sigma/(Vd\Omega)$, where Ω is the solid angle subtended by the detector. Note that q has the units of reciprocal length so scattering at a given q is sensitive to real space inhomogeneities on the scale q^{-1} .

The small- q region required for evaluation of large-scale morphology is not accessible with conventional small-angle x-ray scattering, thus the necessity to use USAXS where scattering angles approach seconds of arc. The USAXS data we present in this work were taken at the UNICAT beam line (33ID) at the Advanced Photon Source (APS) at Argonne National Laboratory. The Bonse-Hart USAXS camera at this facility covers the regime of $10^{-4} \text{ \AA}^{-1} \leq q \leq 0.1 \text{ \AA}^{-1}$. The data were desmeared using routines provided by UNICAT. The incident wavelength was 1 Å.

AC Impedance Spectroscopy. In preparation for impedance measurements, 25-mm X 25-mm squares were cut from cast films of the fibers in epoxy. The squares were then lightly polished to remove any surface and thickness inhomogeneities and to reduce the “skin” layer of epoxy that might insulate the fiber network. Gold was thermally evaporated on the squares using a Denton Explorer® 18 Cryo Auto High Vacuum Deposition System. The squares were sandwiched between two metal washers each with a 20-mm hole that served as templates for depositing circular gold plating on each side of the samples. The plating thicknesses were 1000 Å on each side.

To evaluate the electrical percolation threshold, impedance values were measured using a Novocontrol High-Resolution Dielectric Analyzer provided by the Polymer Branch (MLBP) at Wright Patterson Air Force Base in Dayton, OH. The AC voltage amplitude was

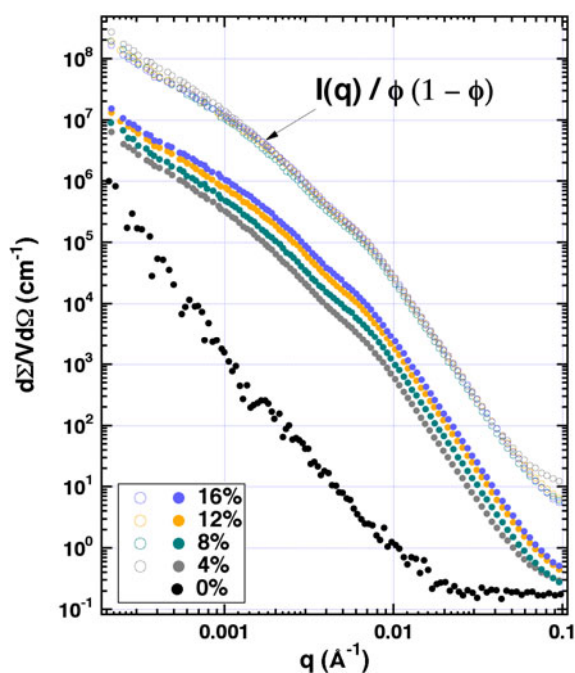


Figure 1. Scattering profiles of ASI PR-19 carbon nanofiber/epoxy composites. The percentages in the legend correspond to nanofiber loading (wt%). The solid symbols correspond to unshifted data on an absolute scale. The open-circle data are $I(q)/\phi(1 - \phi)$, where ϕ is the carbon volume fraction.

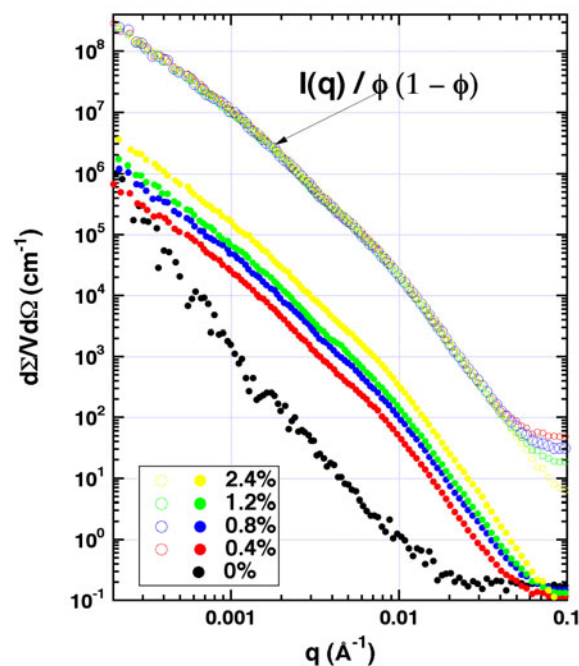


Figure 2. Scattering profiles of lightly loaded ASI PR-19 carbon nanofiber/epoxy composites. The percentages in the legend correspond to nanofiber loading (wt%). The solid symbols correspond to unshifted data on an absolute scale. The open-circle data are $I(q)/\phi(1 - \phi)$, where ϕ is the carbon volume fraction.

V with no DC bias. The frequencies ranged from 10^{-2} to 10^7 Hz, and the measurements were taken at 25°C.

RESULTS AND DISCUSSION

USAXS Data. Initially, we obtained USAXS data for five composites made with varying carbon nanofiber loadings (0, 4, 8, 12, 16-wt%) (Figure 1). The 0%-loaded (pure epoxy) sample was subtracted from each profile. The data in Figure 1 scale as $\phi(1 - \phi)$ where ϕ is the volume fraction of carbon assuming densities of 2.0 g/cm^3 for CNFs and 1.25 g/cm^3 for the epoxy. The observed scaling confirms that the scattering length density contrast ($\Delta\rho^2$) between the fibers and the epoxy is constant. Also, minimal change in profile shape is observed.

To determine if percolation is observable with ultra-small angle scattering, a series of lightly loaded samples (0.4–2.4-wt%) was studied (Figure 2). A 0%-loaded (pure epoxy) background was subtracted from the observed profiles. In Figure 2, the shapes of the curves are similar and scale to higher intensities as the fiber loading is increased, tracking the observations at higher loading. Furthermore, by dividing the intensities by $\phi(1 - \phi)$, we see little change in the shapes of the scattering profiles as the fiber concentration is increased. (Figure 2)

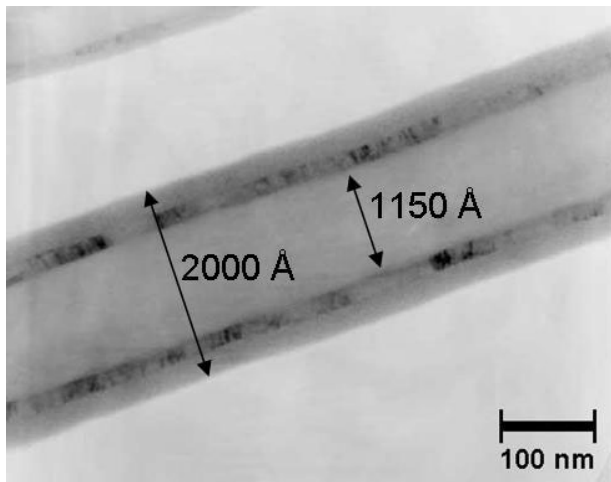


Figure 3. TEM image of an ASI carbon nanofiber suspended in epoxy. The fiber shown has a radius = 1000 Å, and a shell thickness = 425 Å.

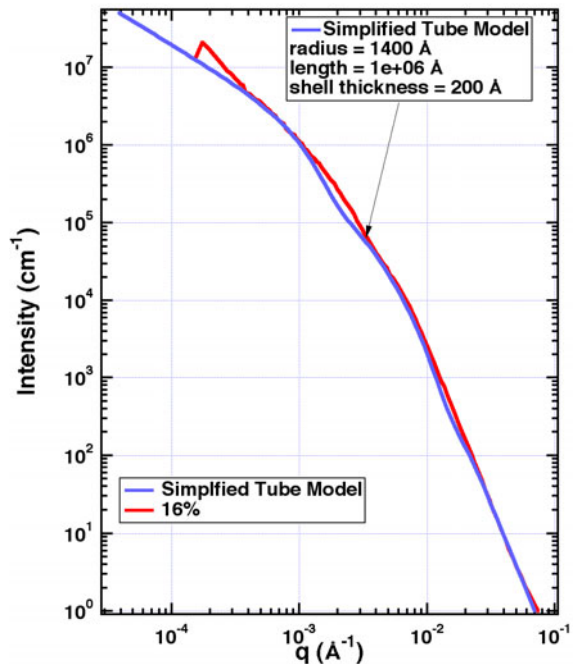


Figure 4. Simplified tube model vs. 16% PR-19/Epon862/W. Parameters used in the fit other than what is shown in the figure are: $\rho_{\text{PR-19}} = 2.0 \text{ g/cm}^3$, $\rho_{\text{Epon862/W}} = 1.25 \text{ g/cm}^3$, $(\Delta\rho^2) = 3.16 \times 10^{21} \text{ (cm}^{-4}\text{)}$, $\phi = 0.11$. Note that ϕ was calculated assuming a density of 2.0 g/cm^3 for carbon due to the tube assumption applied to the fibers.

Further analysis of these data led to an understanding of the fiber dimensions. We utilized a simplified tube model to approximate the scattering fiber form factor. This simplified model matches the exact tube form factor when the tube wall is thin, but the model suppresses the minima that are seen in the exact form factor since minima are seldom seen in the measured data. This simplified model is inadequate to fit the data rigorously, but we do get approximate dimensions by matching the intensity. We also generalized the simplified tube model to include long-range fractal correlations (not shown), which improves the fit. Further explanation of the details and applications of the simplified tube model will be discussed elsewhere.

Figure 3 shows a transmission electron microscopy (TEM) image of a carbon nanofiber with an outer radius, $r_o = 1000 \text{ Å}$, and a shell thickness, $t = 425 \text{ Å}$. Using these dimensions as an estimate we generated the fit in Figure 4. The tube radius of 1400 Å in Figure 4 is slightly large for isolated nanofibers, however it is well known that fiber dimensions are not consistent from batch to batch. Also, scattering is volume-sensitive and strongly weights large-radius fibers. By comparing the dimensions of Figure 4 to the calculated dimensions from Figure 3, we see that model results are reasonable. The difference between the fit and the data at low- q values in Figure 4 indicates the tube wall is less than 425 Å and that the tubes are aggregated on larger length scales. Nevertheless, the fact that a monodisperse tube model fits reasonably well indicates good CNF dispersion on the probed length scale.

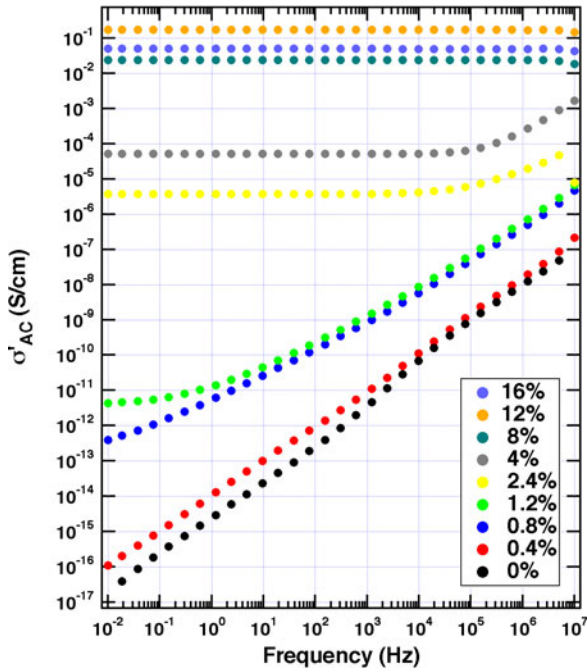


Figure 5. Specific bulk AC conductivity vs. frequency. The data are reported in carbon weight percentages. From these data, the electrical percolation transition is estimated to be approximately 0.8 – 1.2-wt%.

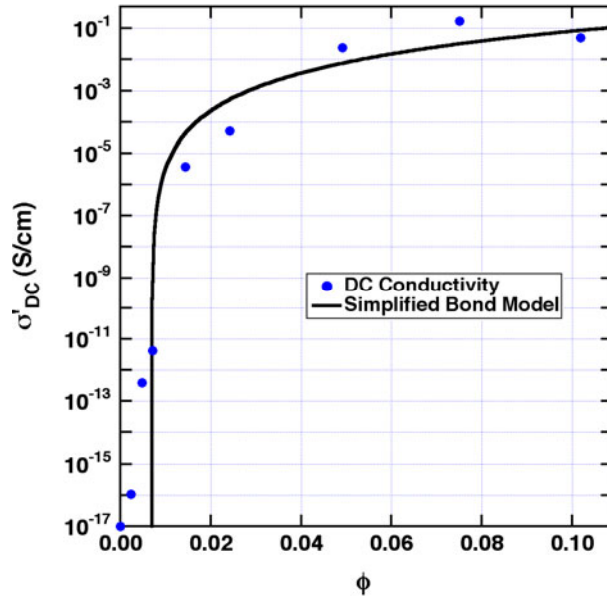


Figure 6. DC bulk conductivity (σ_{DC}) vs. volume fraction (ϕ). The data (blue circles) were determined from the AC data in Figure 5. The simplified bond percolation model (black line) was generated using Eq. 2. The model utilized the following parameters: $\phi_c = 0.007$, $t = 3$.

AC Conductivity Analysis. Figure 5 is a log-log plot of specific bulk AC conductivity against frequency as a function of fiber loading. The percentages shown in Figure 5 are wt%. At loadings $\leq 0.8\%$, the composites show purely insulating behavior, indicated by the slope = 1 in the figure. As concentrations are increased to values $1.2\% \leq \text{wt}\% \leq 4\%$, the samples become conductive, showing an increase in conductivity proportional to fiber loading. At concentrations $4\% < \text{wt}\% \leq 16\%$, the composites show ohmic behavior, with values for the conductivity on the order of 10^{-1} (S/cm). The conductive character of these samples is attributed to an agglomerated network of fiber clusters that form conductive networks during the curing of these composites. From these data, we can estimate the loading concentration at which percolation occurs to be approximately 0.8 – 1.2-wt%.

To better calculate the percolation concentration, the data were analyzed as a function of volume fraction (ϕ) by estimating a density of $\rho = 2.0 \text{ g/cm}^3$ for the carbon fibers. The data were fit using a simplified bond percolation model⁶ to determine the critical filler concentration (ϕ_c) and the conductivity exponent t where

$$\sigma_{DC} \propto |\phi - \phi_c|^t \quad \forall \phi > \phi_c \quad (\text{Eq. 2})$$

and σ_{DC} is the specific DC conductivity. Figure 6 shows the resulting fit using Eq. 2. Comparison of the data to the model yield a percolation threshold is $\phi_c = 0.007$, which is very close to 1.2-wt % ($\phi = 0.0072$), and a conductivity exponent of $t = 3$. This value of t matches the mean-field theory value of $t = 3$.⁷ Furthermore, Koerner et al., using a DC four-

point probe test and based on the same simplified bond percolation model⁶ reported network formation at 0.1-wt% ($\phi_c = 0.005$) for a dispersion of ASI CNF ($\rho_{\text{CNT}} \sim 2.1 \text{ g/cm}^3$) in polyurethane ($\rho_{\text{PU}} \sim 1.19 \text{ g/cm}^3$).⁷ Ultimately, the low value calculated for $\phi_c = 0.007$ is consistent with relatively good dispersion of the fibers.

CONCLUSIONS

The observed scattered intensity is consistent with good fiber dispersion, even though we find no signature of rod-like morphology (power-law slopes of -1) in the q -range explored. In the q -range visible with USAXS, we are unable to see a morphological transition that could be attributed to the formation of a percolated network. Being a topological transition, percolation is not expected to substantially alter the scattering profiles. As the tubes overlap, however, we do expect suppressed intensity at small- q . Based upon the analyses presented, however, we determined the CNFs to be well dispersed on the measured length scale.

From AC impedance spectroscopy, we determined an electrically conductive network is formed throughout the volume of the samples at loadings between 0.8 – 1.2-wt%. Further analysis using the simple bond-percolation model shows the critical volume fraction of CNFs (ϕ_c) = 0.007, which is consistent with the literature and that the samples are relatively well dispersed.

ACKNOWLEDGEMENTS

We thank Pete Jemian and Jan Ilavsky for assistance in collection of the USAXS data. The UNICAT facility at the Advanced Photon Source (APS) is supported by the U.S. DOE under Award No. DEFG02-91ER45439, through the Frederick Seitz Materials Research Laboratory at the University of Illinois at Urbana-Champaign, the Oak Ridge National Laboratory (U.S. DOE contract DE-AC05-00OR22725 with UT-Battelle LLC), the National Institute of Standards and Technology (U.S. Department of Commerce) and UOP LLC. The APS is supported by the U.S. DOE, Basic Energy Sciences, Office of Science under contract No. W-31-109-ENG-38. Work at the University of Cincinnati was supported by the Air Force Research Laboratory through the WBI Program and the University of Dayton Research Institute. The facilities of the Manuel Lujan Jr. Neutron Scattering Center are gratefully appreciated. This work was supported in part by the Office of Basic Energy Science, U.S. Department of Energy

REFERENCES

1. Shofner, M. L.; Lozano, K.; Rodriguez-Macias, F. J.; Barrera, E. V. *Journal of Applied Polymer Science* **2003**, *89*, 3081.
2. Cortes, P.; Lozano, K.; Barrera, E. V.; Bonilla-Rios, J. *Journal of Applied Polymer Science* **2003**, *89*, 2527.
3. Zeng, J.; Saltysiak, B.; Johnson, W. S.; Schiraldi, D. A.; Kumar, S. *Composites Part B. Engineering* **2004**, *35*, 245.
4. Kumar, S.; Doshi, H.; Srinivasarao, M.; Park, J. O.; Schiraldi, D. A. *Polymer* **2002**, *43*, 1701.
5. Thostenson, E. T.; Chunyu, L.; Chou, T. W. *Composites Science and Technology* **2005**, *65*, 491.

6. Stauffer, D.; Aharony, A.; Introduction to percolation theory. London; Washington, DC: Taylor & Francis, **1992**.
7. Koerner, H.; Liu, W. D.; Alexander, M.; Mirau, P.; Dowty, H.; Vaia, R. A. *Polymer* **2005**, 46, 4405.